

# Quantitative Proteomic Study Reveals Amygdalin Alleviates Liver Fibrosis Through Inhibiting mTOR/PDCD4/JNK Pathway in Hepatic Stellate Cells

Hui Huang<sup>1,2,\*</sup>, Su-Jie Ru<sup>3,\*</sup>, Jia-Mei Chen<sup>4,5,\*</sup>, Wei Liu<sup>4,5</sup>, Shan-Hua Fang<sup>2</sup>, Qian Liu<sup>2</sup>, Qian Meng<sup>2</sup>, Ping Liu<sup>4-6</sup>, Hu Zhou<sup>1-3,7</sup>

<sup>1</sup>School of Pharmaceutical Science and Technology, Hangzhou Institute for Advanced Study, University of Chinese Academy of Sciences, Hangzhou, People's Republic of China; <sup>2</sup>Department of Analytical Chemistry, State Key Laboratory of Drug Research, Shanghai Institute of Materia Medica, Chinese Academy of Sciences, Shanghai, People's Republic of China; <sup>3</sup>School of Chinese Materia Medica, Nanjing University of Chinese Medicine, Nanjing, Jiangsu, People's Republic of China; <sup>4</sup>Institute of Liver Diseases, Key Laboratory of Liver and Kidney Diseases (Ministry of Education), Shuguang Hospital Affiliated to Shanghai University of Traditional Chinese Medicine, Shanghai, People's Republic of China; <sup>5</sup>Shanghai Key Laboratory of Traditional Chinese Medicine, Shanghai, People's Republic of China; <sup>6</sup>Institute of Interdisciplinary Integrative Medicine Research, Shanghai University of Traditional Chinese Medicine, Shanghai, People's Republic of China; <sup>7</sup>University of Chinese Academy of Sciences, Beijing, People's Republic of China

\*These authors contributed equally to this work

Correspondence: Hu Zhou, Shanghai Institute of Materia Medica, Chinese Academy of Sciences, 555 Zuchongzhi Road, Shanghai, People's Republic of China, Email [zhouhu@simm.ac.cn](mailto:zhouhu@simm.ac.cn); Ping Liu, Shuguang Hospital affiliated to Shanghai University of Traditional Chinese Medicine, Shanghai, People's Republic of China, Email [liliver@vip.sina.com](mailto:liliver@vip.sina.com)

**Purpose:** Hepatic fibrosis is a major cause of morbidity and mortality for which there is currently limited therapy. Amygdalin, a cyanogenic glucoside derived from *Semen Persicae*, exerts significant anti-fibrotic effects in the liver. However, the molecular mechanism by which amygdalin inhibits the progression of liver fibrosis remains unclear. This study aimed to elucidate the potential mechanism of action of amygdalin against liver fibrosis.

**Methods:** Quantitative proteomic profiling of the mouse liver tissues from control, carbon tetrachloride (CCl<sub>4</sub>)-induced fibrosis, and amygdalin-treated groups was performed to explore the key effector proteins of amygdalin. Histology and immunohistochemistry as well as serum biochemical analysis were performed to evaluate amygdalin efficacy in mice. The key gene programmed cell death protein 4 (PDCD4) was overexpressed or knocked down in human hepatic stellate cells (HSCs). The mRNA and protein levels of related molecules were detected by RT-qPCR and Western blotting, respectively.

**Results:** Amygdalin could effectively ameliorated CCl<sub>4</sub>-induced liver fibrosis in mice. Bioinformatics analysis revealed that PDCD4 was downregulated in CCl<sub>4</sub>-induced liver fibrosis, but amygdalin treatment reversed these changes. An in vitro study showed that PDCD4 inhibited the activation of human hepatic stellate cell line LX-2 cells by regulating the JNK/c-Jun pathway and amygdalin inhibited the activation of LX-2 cells in a PDCD4-dependent manner. We further found that amygdalin inhibited the phosphorylation of PDCD4 at Ser67 by inhibiting the mTOR/S6K1 pathway to enhance PDCD4 expression.

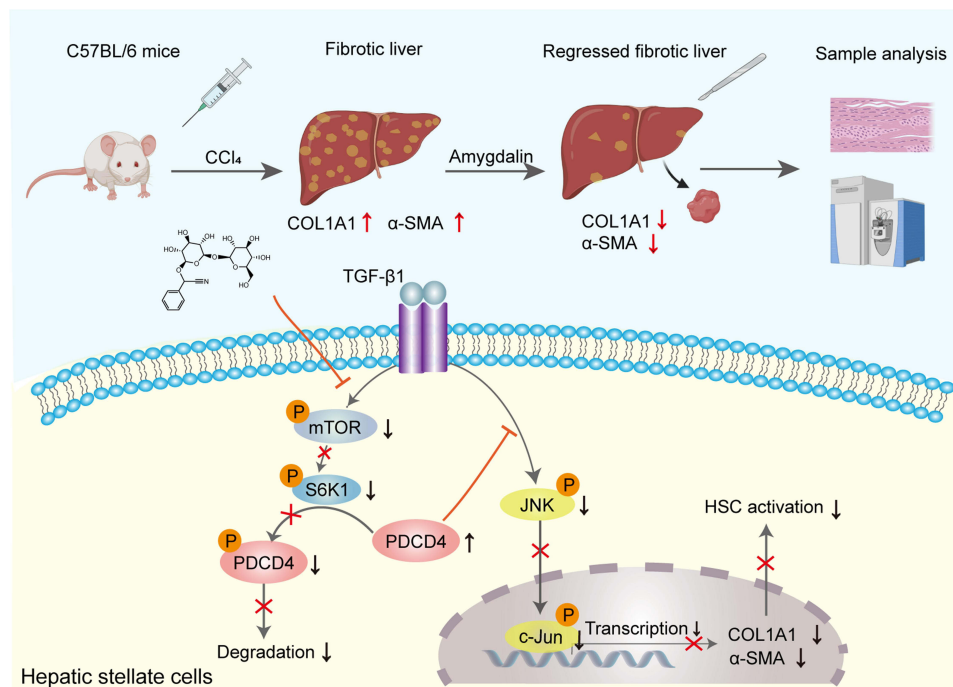
**Conclusion:** Our data demonstrated a potential pharmaceutical mechanism by which amygdalin alleviates liver fibrosis by inhibiting the mTOR/PDCD4/JNK pathway in HSCs, suggesting that PDCD4 is a potential target for the treatment of liver fibrosis.

**Keywords:** amygdalin, PDCD4, HSC activation, proteomics, mTOR/S6K1

## Introduction

Chronic liver diseases are a major global health burden and account for approximately 2 million deaths per year worldwide.<sup>1</sup> Liver fibrosis is a late stage process of many chronic liver diseases including viral infection, alcohol consumption, drug abuse, fatty liver, steatohepatitis, parasitic infection and autoimmune disease.<sup>2,3</sup> Fibrosis is a reversible wound-healing response characterized by the accumulation of excessive extracellular matrix (ECM) following liver injury, which may further lead to cirrhosis accompanied by liver failure or liver cancer.<sup>4</sup> Transforming growth factor-

## Graphical Abstract



beta (TGF-β) mediated hepatic stellate cell (HSC) activation is considered a critical event that drives ECM assembly and remodeling, synergistically promoting fibrosis. However, the complex mechanisms of HSC activation in TGF-β1-mediated liver fibrosis remain incompletely understood. Therefore, it is urgent to identify key mediators involved in this process to develop more effective strategies for treating liver fibrosis.

The TGF-β1-mediated Smad signaling is a well-established canonical profibrotic pathway, whose activation can lead to the upregulation of key markers of fibrosis such as alpha-smooth muscle actin (α-SMA) and type I collagen α1 (COL1A1), both of which are critical indicators of ECM remodeling and myofibroblast activation.<sup>5</sup> However, since TGF-β1/Smad is also involved in essential physiological process such as immune regulation and tissue repair, therapies specifically targeting this pathway are not yet available for clinical use.<sup>6</sup> Recently, the role of TGF-β1-mediated other signaling pathways such as mitogen-activated protein kinase (MAPK), phosphoinositide 3-kinase/AKT, mammalian target of rapamycin (mTOR) and GTPase pathways in the development of liver fibrosis has gradually been understood.<sup>7–10</sup> Therefore, understanding the physiological and targetable regulators of downstream of TGF-β1 is important for the prevention and treatment of liver fibrosis.

Amygdalin is a natural cyanide found in the seeds of Rosaceae species such as almond, apricot, and apple seeds.<sup>11</sup> It was reported to have anti-inflammatory, antioxidant, anti-inflammatory, anti-neoplastic and anti-fibrotic effects.<sup>12–15</sup> Recent study found that amygdalin ameliorates renal and liver fibrosis mainly by suppressing TGF-β1/Smad signaling pathway and regulating the key enzymes of ECM degradation – Matrix Metalloproteinases-9 (MMP-9) and tissue Inhibitor of Metalloproteinases 1 (TIMP-1).<sup>16,17</sup> In addition, as an active ingredient of Fuzheng Huayu formula, which is a NMPA (National Medical Products Administration)-approved anti-fibrotic medicine in China, amygdalin is effective at alleviating liver fibrogenesis by inhibiting the proliferation and collagen production of active HSC, HSC activation and hepatocyte apoptosis.<sup>18–24</sup> However, due to the herbal products having multi-modulatory and multi-target action, comprehensive mechanism of anti-fibrotic effects of amygdalin remains elusive.<sup>25</sup>

Programmed cell death protein 4 (PDCD4) is a tumor suppressor protein that has been implicated in various cellular processes, including apoptosis, cell proliferation, and stress responses.<sup>26</sup> Recent research has suggested that PDCD4 also plays a role in fibrosis, particularly in regulating the hepatic and renal fibrosis development via MiR-21/PDCD4/AP-1

feedback loop.<sup>27–31</sup> What's more, PDCD4 has been reported to interact with cellular signaling pathways, including the PI3K/Akt and MAPK pathways, both of which are involved in cell survival, proliferation, and fibrotic responses.<sup>32–34</sup> While the role of PDCD4 in liver fibrosis is still being explored, its potential as a therapeutic target is gaining interest.

In this study, with a proteomic approach, we found that PDCD4 was a potential target of liver fibrosis and functions as an inhibitor of the c-jun N-terminal kinase (JNK) signaling pathway. Amygdalin upregulates PDCD4 by inhibiting mTOR/S6K1 phosphorylation, thereby inhibiting HSC activation induced by TGF- $\beta$ 1. Our results may provide new insights into the noncanonical TGF- $\beta$ 1 signaling-targeted therapies for liver fibrosis.

## Materials and Methods

### Animal Experiments

In the animal experiment, C57BL/6 mice (male, 8 weeks, 18–20 g) were obtained from the Shanghai SLAC Laboratory Animal Co. Ltd. (China) and housed under the same standard conditions. To induce chronic hepatic fibrosis, mice were injected intraperitoneally (i.p.) with 2 mL/kg CCl<sub>4</sub> in a 1:10 ratio with olive oil twice weekly for a total of 5 weeks. From the third week of CCl<sub>4</sub> exposure, mice in the amygdalin treatment group (CCl<sub>4</sub> + Amy group) were administered 100 mg/kg amygdalin (dissolved in saline), and mice in the model group (CCl<sub>4</sub> group) were administered an equal volume of saline daily by oral gavage for further 3 weeks. Mice in the control group were injected with olive oil and fed with saline in the same manner as described above. After 5 weeks, all the mice were sacrificed. Blood samples were stored at 4°C for 40 min until the next procedures. Liver tissue was harvested and cut in half. One half was stored at –80°C after being quickly frozen in liquid nitrogen, and the other half prepared for Formalin-fixed paraffin-embedded (FFPE) samples. All animal experiments were reviewed and approved by the Experimental Animal Ethics Committee of Shanghai University of Traditional Chinese Medicine (No. 20140005) and conducted according to the AAALAC guidelines.

### Histology and Immunohistochemistry

A piece of liver tissue fixed with formalin was embedded in paraffin and sliced into 5  $\mu$ m sections that were stained with H&E and Masson's trichrome for a histological examination. Immunohistochemistry with  $\alpha$ -SMA antibody (at a 1:100 dilution in PBS) was performed. The histological changes were evaluated by using optical microscopy (Olympus BX51, Japan) in 200 histological fields. The Image J software was used to quantify the degree of fibrosis.

### Serum Biochemical Analysis

The enzymatic activities of Alanine Transaminase (ALT) and Aspartate Aminotransferase (AST) were measured, using an ALT Activity Assay Kit (Cat. ab105134, Abcam) and the AST Activity Assay Kit (Cat. ab138878, Abcam) according to the manufacturer's instructions. ALT and AST activities were measured at OD450 and OD570 nm, respectively, using a colorimetric analyzer (Dri-Chem 3000, Fuji Photo Film, Japan).

### Cell Culture and Treatment

Human hepatic stellate cell line LX-2 cells (Procell Life Science & Technology, CL-0560) and mouse HSC cell line JS1 cells (provided by laboratory of Liu, Shanghai University of Traditional Chinese Medicine) were cultured in DMEM medium containing 10% fetal bovine serum (FBS) at an environment of 37°C with 5% CO<sub>2</sub>. Cells were treated with increasing concentrations of amygdalin for 12 h and then stimulated with 5 ng/mL TGF- $\beta$ 1 (R&D Systems) for another 24 h. Dimethyl sulfoxide (DMSO) was used as a control.

### RNA Isolation and Quantitative Real-Time PCR (RT-qPCR)

Total RNA was extracted from the LX-2 cells using TRIzol reagent (Sigma, USA) and subjected to reverse transcription using the PrimeScript RT Reagent Kit (Takara, Japan), following the manufacturer's protocol. Quantitative PCR was performed using the Thunderbird SYBR Green qPCR Mix reagent (Toyobo) on a 7500 Fast Real-Time PCR system (Applied Biosystems, Irvine, CA). All runs were performed in triplicate and the GAPDH gene served as an endogenous control for normalization. The primer sequences used were as follows: PDCD4: 5'-ATGGATGTAGAAAATGAGCAG-3', 5'-TTAAAGTCTTCTCAAATGCCC-3';

ACTA2: 5'-CGTGGCTATTCCTTCGTTAC-3', 5'-TGCCAGCAGACTCCATCC -3'; COL1A1: 5'-CCGTGACCTCAAGATGTGCCACT-3', 5'-TCATGCTCTCGCCGAACCAG-3'; GAPDH: 5'-GGTATCGTGGAAGGACTCATGAC-3', 5'-ATGCCAG-TGAGCTTCCCGTTTCAGC-3'.

## siRNA and Plasmid Transfection Experiments

The siRNA targeting human PDCD4 (siRNA: 5'-3':AAGGUGGCUGGAACAUCUATT) was synthesized by Genepharma Co. (Shanghai, China). Human PDCD4 was cloned into pCMV6-XL5 vector and purchased from OriGene Technologies Inc. (Rockville, MD, USA). LX-2 cells were cultured in 24 well plates and transfected with 100 nM PDCD4 siRNA or 500 ng PDCD4 plasmid for 48 h using Lipofectamine 3000 and Plus reagents according to the manufacturer's protocols (Invitrogen Corp., Carlsbad, CA). After 6 hours of transfection, the medium was replaced with fresh DMEM medium containing 10% fetal bovine serum, and cells were harvested after 72 h using a cell lysis buffer to perform Western blot analysis.

## Western Blot Analysis

Liver tissues or cell samples were collected with SDT lysis buffer (4% SDS, 0.1 M Tris-HCl (pH 7.6), 0.1 M DTT). The lysates were boiled for 10 min at 95°C and then soluble fractions were isolated by centrifugation at 4°C, 12,000 g for 20 min. Proteins were separated on 10% SDS-PAGE gels and transferred to polyvinylidene difluoride (PVDF) membranes (Millipore), which were then blocked with 5% bovine serum albumin (BSA) for 1 h and subsequently incubated with primary antibodies overnight at 4°C. The following morning, the membranes were washed 3 times with TBST buffer (8 g/L NaCl, 200 mM Tris, 0.1% Tween 20, pH 7.4), and incubated with the secondary antibodies for 1 h at room temperature. The blots were scanned using a SmartChemi 610 (Beijing sagecreation). Each experiment was repeated at least three times, and the images were analyzed using ImageJ software. The following primary antibodies: COL1A1 (CST, #72026),  $\alpha$ -SMA (Abcam, ab5694), PDCD4 (CST, #9535), phospho-PDCD4 (Ser67) (Invitrogen, PA5-105015), mTOR (CST, #2972), phospho-mTOR (Ser2448) (CST, #5536), S6K1 (CST, #9202), phospho-S6K1 (Thr421/Ser424) (CST, #9204), JNK (Santa Cruz, sc-7345), phospho-JNK (Thr183/Tyr185) (Santa Cruz, sc-6254), c-Jun (CST, #9165), phospho-c-Jun (Ser73) (CST, #3270) and GAPDH (Sigma-Aldrich, G9545).

## Protein Extraction and Sample Preparation

Liver tissues dissected from a total of 15 mice among three groups were lysed in SDT lysis buffer, the lysates were homogenized with sonication, denatured for 10 min at 95°C and centrifuged at 12,000 g for 10 min. The supernatants were collected, and the protein concentration was determined by the tryptophan-based fluorescence quantification method.<sup>35</sup> Subsequently, 100  $\mu$ g proteins from each sample were digested with trypsin following the filter-assisted sample preparation (FASP) experiment as described previously.<sup>36</sup>

## LC-MS/MS Analysis

The LC-MS/MS analysis was performed on an LTQ Orbitrap Elite (Thermo Fisher Scientific) platform connected to an online nanoflow EASYnLC1000 hPLC system (Thermo Fisher Scientific). Peptides were loaded on a self-packed column (75  $\mu$ m  $\times$  15 cm, C18-AQ 3  $\mu$ m, 120Å beads, Dr Maisch GmbH, Ammerbuch, Germany) and separated with a 240 min gradient for each sample at a flowrate of 300 nL/min. The mobile phase A of RP-HPLC was 0.1% formic acid in water, and the mobile phase B was 0.1% formic acid in acetonitrile. The mobile phase gradient conditions were as follows: 5% B for 1 min; 30% B for 234 min; 85% B for 235 min; 100% B for 240 min; Data-dependent acquisition (DDA) mode was performed using Xcalibur software in positive ion mode. The MS1 full scan was set at a resolution of 60,000 by Orbitrap mass analyzer (300–1800 m/z) and the top 15 precursor ions were selected for MS2 scan by HCD fragmentation at a resolution of 17,500.

## Database Searching

Raw files acquired from LC-MS/MS were analyzed with MaxQuant software (version 1.6.5.0) by searching against the UniProt Mus musculus database (downloaded from <http://www.uniprot.org>). Carbamidomethyl cysteine was searched as

a fixed modification, oxidized methionine and protein N-term acetylation as variable modifications. Trypsin digestion was defined with cut-sites at K/R except when followed by P (Trypsin/P). The maximum missing cleavage site was set as 2. The tolerances of first search and main search for peptides were set at 20 ppm and 4.5 ppm, respectively. Label-free quantification (LFQ) method was used for the measurement of relative protein abundances across different samples. The false discovery rate (FDR) was set to 0.01 for both peptide and protein identification. Other database search parameters are the default values of the software system.

## Proteomic Data Analysis

The proteins identified were filtered to eliminate the identifications from the common contaminants and reverse database. Only proteins which contain at least 1 unique peptide were used for subsequent analysis. Protein intensities were normalized using the median centering method across total proteins to correct sample loading differences. Proteins with more than 50% missing values were excluded to make sure that each sample had enough data for imputation. K-nearest neighbor (k-NN) imputation was performed in R software to fill the missing values of protein abundances. One way analysis of variance (ANOVA) and Tukey's honestly significant difference (HSD) test were conducted for comparative analysis of protein abundance across different groups. The `aov()` function in R software was used to perform ANOVA. Only those proteins with fold change  $>1.5$  or  $<0.67$  and P value  $<0.05$  were considered as the significantly changed proteins. The proteins with significant expression change between CCl<sub>4</sub> and Amygdalin treatment group were clustered by Fuzzy C-means method using Mfuzz package in R software. The optimal parameter values of clusters "c" and fuzzification parameter "m" were set as 4 and 3, respectively. The abundance correlation of proteins between any two samples was assessed using the Pearson method with "corrplot" package.<sup>37</sup> For Gene Set Enrichment Analysis (GSEA), gene name of mice from raw data were mapped to corresponding human homologues, using homology information from the Mouse Genome Informatics database (The Jackson Laboratory). GSEA of Gene Ontology Biological Process (GOBP) for global proteomic expression data was performed using GSEA software (4.1.0 version, Broad Institute, Massachusetts, USA).<sup>38,39</sup> The Molecular Signature Database (MSigDB) "c5.go.bp.v2023.Hs.symbol" was used, and parameters were set as follows: mPerm=500, minGSSize=10, maxGSSize=500. GO terms enriched with FDR  $< 0.25$  were considered to be significant, and the top 15 enriched GO terms were listed in our data. The BioRender software was used to draw proteomic flow chart and drug mechanism diagram.

## Statistical Analysis

Statistical analysis was performed using GraphPad Prism 9 (GraphPad Software, CA), and the biological experimental data were presented as the mean  $\pm$  SD. One-way ANOVA followed by Tukey's HSD test was performed for multiple comparison analyses between groups of samples, as it allows for pairwise comparisons while controlling for type I error rates. Two-sided P values  $<0.05$  were considered statistically significant.

## Results

### Amygdalin Ameliorates Liver Fibrosis and Induces the Expression of PDCD4 in the CCl<sub>4</sub>-Induced Liver Fibrosis

First of all, we evaluated the effect of amygdalin ([Supplementary Figure A](#)) on CCl<sub>4</sub>-induced liver fibrosis, and the flow chart of our animal experiment was illustrated in [Figure 1A](#). As shown in [Figure 1B](#), the deposition of collagen as depicted by Masson's staining and  $\alpha$ -SMA were both increased in fibrotic mice, while these two fibrosis markers were visibly less widespread in amygdalin-treated mice. The serum activities of ALT and AST were significantly higher after the CCl<sub>4</sub> exposure and reduced by amygdalin treatment ([Figure 1C](#)). These results indicate that amygdalin administration could effectively eliminate hepatic fibrosis and ameliorate the abnormal liver function induced by CCl<sub>4</sub> in mice.

To further explore the downstream effectors of amygdalin in the fibrotic liver tissue, we conducted quantitative proteomic analysis to investigate the differences in liver proteome profiles between mice under different treatments. Label-free global proteomic analysis of 15 liver tissue samples from control, CCl<sub>4</sub>-fibrosis and amygdalin treatment groups identified a total of 3435 non-redundant proteins ([Figure 2A](#)). Two thousand four hundred and forty-nine proteins

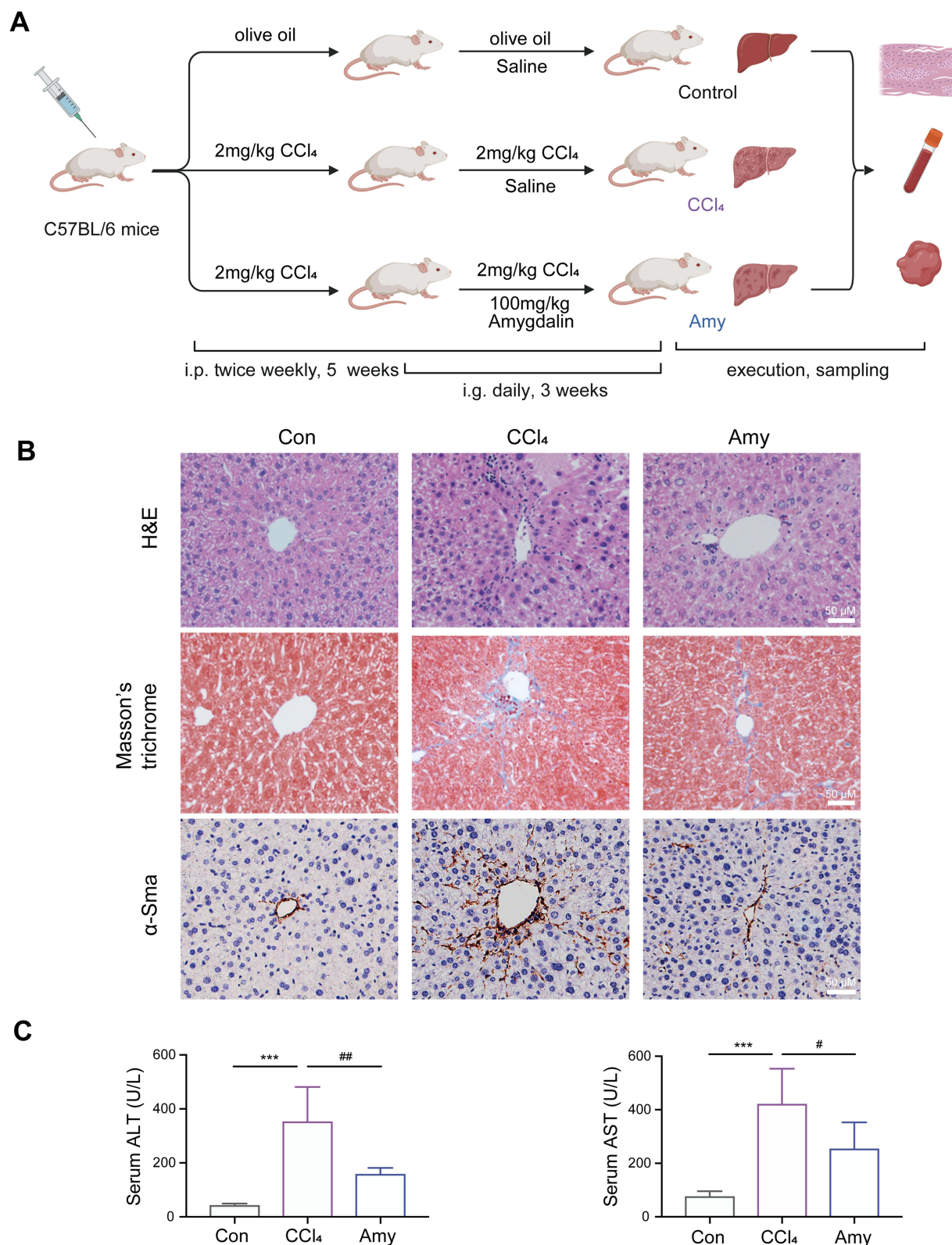


**Figure 1** Anti-fibrotic effect of amygdalin on CCl<sub>4</sub>-induced fibrotic mice models. **(A)** The flow chart of animal experiment. **(B)** Histological analyses of liver tissues from control (Con), CCl<sub>4</sub>-induced fibrosis (CCl<sub>4</sub>), CCl<sub>4</sub> combined with amygdalin treatment (Amy) groups performed using H&E, Masson's trichrome and  $\alpha$ -Sma antibody (scale bar 50  $\mu$ m, 200 $\times$  magnification). **(C)** Biochemical analysis of serum samples in each group. ALT, alanine transaminase; AST, aspartate transaminase. n=5, \*\*\*P < 0.001 vs Con group; #P < 0.05, ##P < 0.01 vs CCl<sub>4</sub> group.

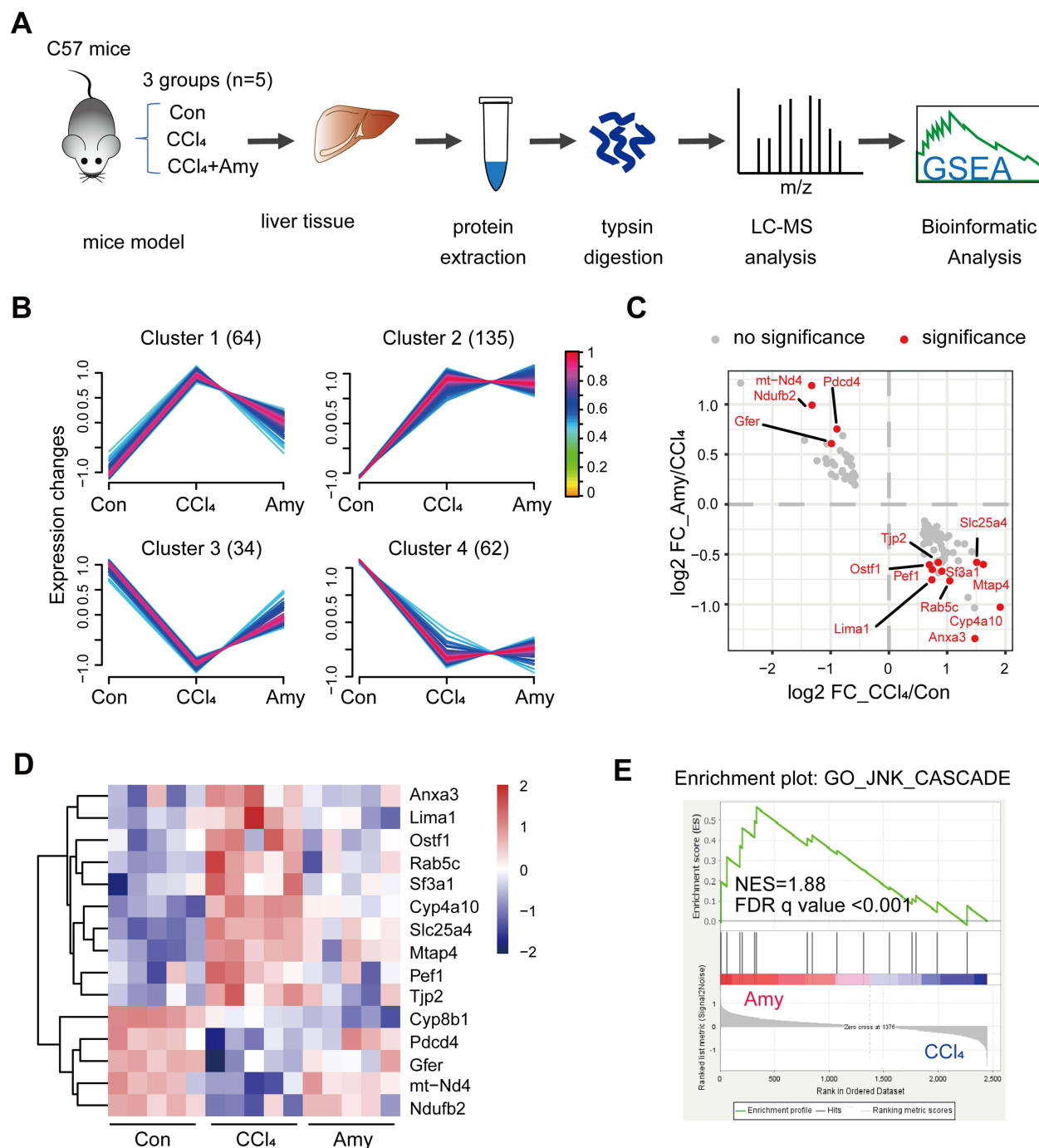


**Figure 2** Proteomic analysis identified PDCD4 as a potential effector protein of amygdalin treatment. **(A)** Workflow chart of label-free quantitative proteomic experiment. **(B)** Clustering of the differentially expressed proteins by fuzzy c-means clustering algorithm. **(C)** Scatterplot of the proteins from in cluster 1 and cluster 3. Red points indicated the proteins that having a significant change in both comparison groups (fold change >1.5 or <0.67 and P <0.05). Gray points indicated proteins that failed to pass the criteria. **(D)** Hierarchical clustering analysis of significantly reversed proteins in amygdalin treatment group as compared to CCl<sub>4</sub> group. Color of each cell represents the expression level of proteins. **(E)** The biological process of JNK\_CASCADE was enriched by GSEA analysis using total identified proteins between CCl<sub>4</sub> and Amy group. **Abbreviation:** NES, normalized enrichment score.

with less than 50% missing data were filled by KNN imputation and used for the following analysis. The correlation coefficient of the intensities between any two cohorts was greater than 0.96 (Supplementary Figure B), demonstrating a good biological reproducibility among each group. With the criteria of fold change >1.5 or <0.67 and P value <0.05, 295 proteins were differentially expressed in CCl<sub>4</sub> group compared with Con group (Supplementary Figure C and

[Supplementary Table 1](#)). Furthermore, based on the protein abundance profile across the three groups, these proteins were categorized to four clusters using Fuzzy C-means method ([Figure 2B](#) and [Supplementary Table 2](#)). Proteins in cluster 1 (64 proteins) and 3 (34 proteins) that changed significantly in CCl<sub>4</sub> group but returned to normal levels by amygdalin treatment were considered to be mainly involved in the anti-fibrotic effect of amygdalin. Among these proteins, only 14 proteins as showed in [Figure 2C](#) and [D](#) were significantly reversed by amygdalin. In addition, gene set enrichment analysis (GSEA) between CCl<sub>4</sub> and amygdalin group showed that the pathways related to lipid metabolic process, NTP biosynthetic process and MAPK cascade were upregulated, whereas pathways associated with the vesicle transport, immunity and membrane permeability were downregulated ([Supplementary Table 3](#)). The above results suggest that amygdalin may influence the progression of liver fibrosis by regulating these pathways. Notably, we observed that proteins associated with JNK cascade were significantly increased in the liver of amygdalin-treated group ([Figure 2E](#) and [Supplementary Table 3](#)). Among them, PDCD4, one of leading-edge protein in JNK cascade pathway, was significantly decreased in the CCl<sub>4</sub>-induced fibrosis group as compared to control group, and amygdalin treatment restored the PDCD4 protein level by 1.69 fold ([Figure 3A](#) and [Supplementary Table 4](#)). Previous studies have reported that knockdown of PDCD4 leads to JNK activation and may also regulate cell survival through its interaction with the JNK signaling pathway.<sup>40–42</sup> The subsequent Western blot analysis verified this change in PDCD4 expression in three different groups ([Figure 3B](#)), indicating that the PDCD4 might play an important role in the amygdalin inhibition of liver fibrosis.

## Amygdalin Inhibits TGF- $\beta$ 1-Induced HSC Activation and Upregulates PDCD4 Expression in the HSCs

HSC activation is a key event in fibrogenesis and can be reproduced in vitro by prolonged culture on plastic or stimulated by TGF- $\beta$ 1 treatment. Therefore, we examined PDCD4 expression in human HSC cell line LX-2 cells under the condition of TGF- $\beta$ 1 and/or amygdalin treatment. Both of the RT-qPCR and Western blotting assay revealed that amygdalin treatment significantly downregulated the expression of the fibrogenic markers ( $\alpha$ -SMA and COL1A1) induced by TGF- $\beta$ 1 in a concentration-dependent manner ([Figure 4A](#) and [B](#)). However, PDCD4 expression was distinctly decreased by the TGF- $\beta$ 1 stimulation and was restored by amygdalin treatment only at the protein level ([Figure 4B](#) and [Supplementary Figure D](#)). The mRNA level of PDCD4 was not changed either by TGF- $\beta$ 1 or amygdalin ([Figure 4A](#)). To determine whether the anti-fibrotic effect of amygdalin depends on PDCD4 in HSCs, we knocked down the PDCD4 gene using PDCD4 siRNA. We found that the inhibitory effect of amygdalin on TGF- $\beta$ 1-induced activation of LX-2 cells was obviously abolished when the expression of PDCD4 was silenced ([Figure 4C](#)). These results suggested that amygdalin inhibits TGF- $\beta$ 1-induced HSC activation via regulating protein expression of PDCD4.

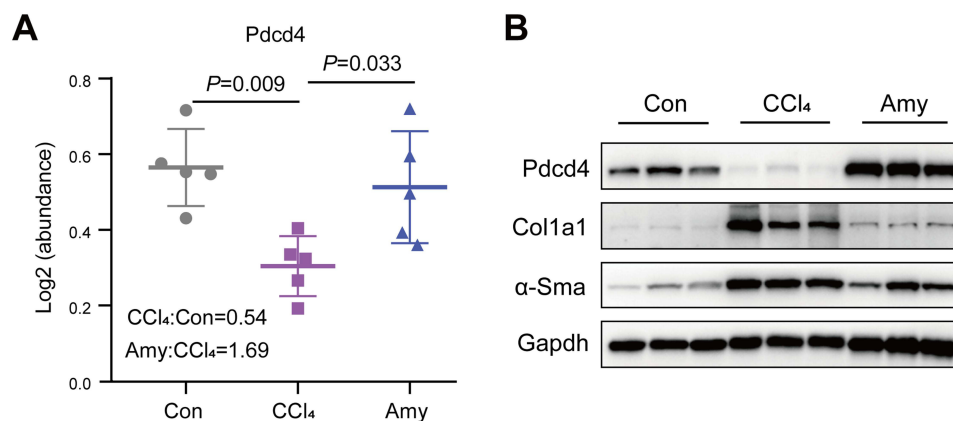


**Figure 3** The expression level of PDCD4 in liver tissues of mice. **(A)** Boxplot showing the log<sub>2</sub> transformed abundance of Pdc4, as quantified by LC-MS/MS. **(B)** Western blot of Pdc4,  $\alpha$ -Sma and Col1a1 protein expression in liver tissues.

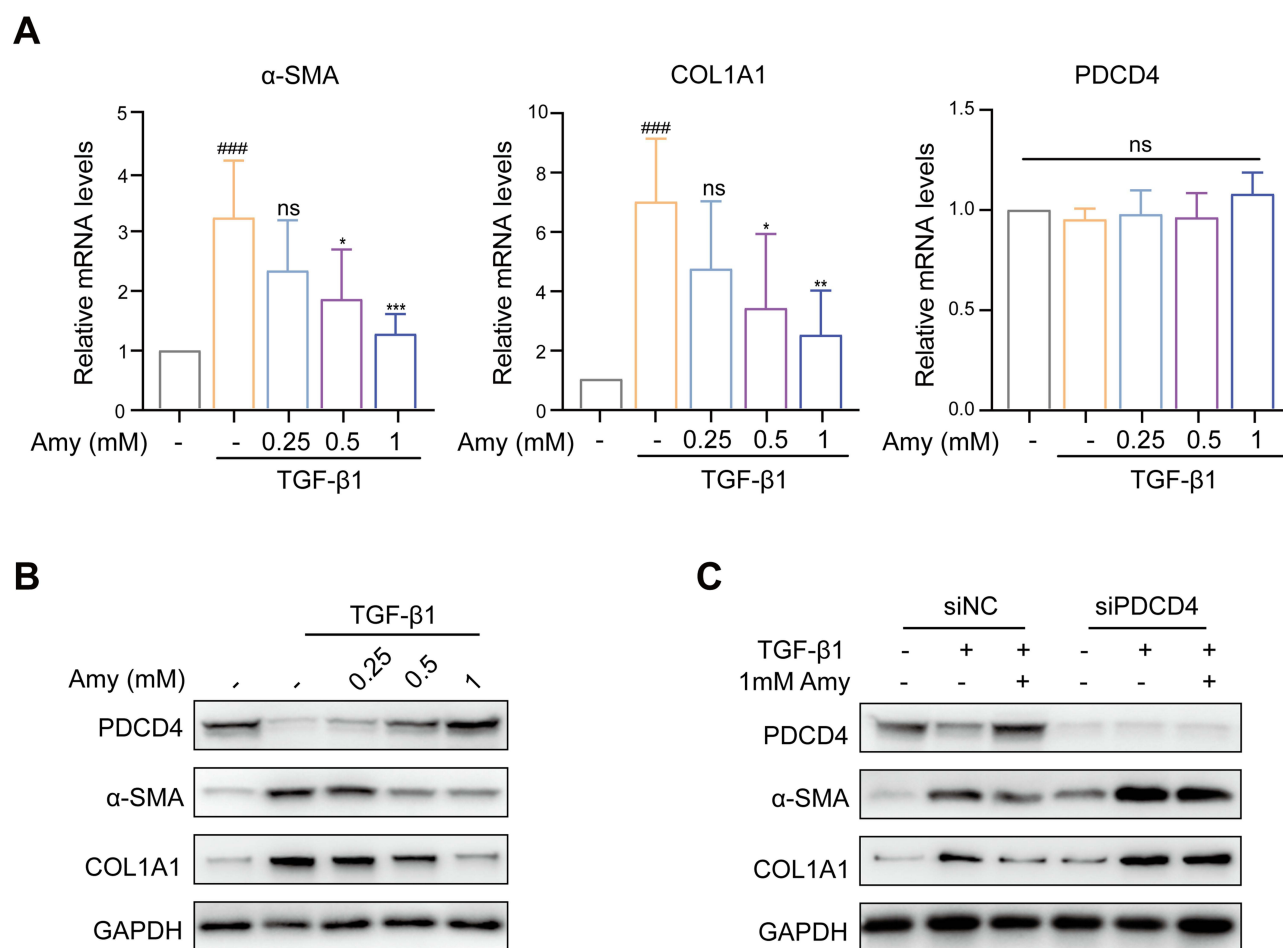


**Figure 4** The role of PDCD4 in mediating the antifibrotic effects of amygdalin. **(A)** LX-2 cells were treated with amygdalin for 12 h and stimulated with TGF-β1 for another 24 h. Relative mRNA expression was measured by rt-qPCR for α-SMA, COL1A1 and PDCD4.  $n = 5$ , ##### $P < 0.001$  vs control group, \* $P < 0.05$ , \*\* $P < 0.01$ , \*\*\* $P < 0.001$  vs TGF-β1 group; ns indicates no significance. **(B)** The results of Western blot for PDCD4, α-SMA and COL1A1 protein expression. **(C)** LX-2 cells transfected with siNC or siPDCD4 were treated with amygdalin for 12 h and further stimulated with TGF-β1 for another 24 h. The protein levels of PDCD4, α-SMA and COL1A1 were analyzed by Western blotting.

## PDCD4 Inhibits HSC Activation and Negatively Regulates JNK Signaling Pathway

As PDCD4 protein was downregulated in TGF-β1-activated HSC cells, we additionally introduced PDCD4 into the HSC cell line LX-2 cells to investigate the function of PDCD4. When LX-2 cells were overexpressed with PDCD4, the TGF-β1-stimulated expression of α-SMA and COL1A1 were significantly decreased (Figure 5A and B). As PDCD4 is involved in the regulation of JNK signaling pathway as indicated by GSEA analysis, we also examined the role of PDCD4 in this pathway. We observed that PDCD4 overexpression inhibited phosphorylation of JNK (p-JNK) and downstream c-Jun (p-c-Jun) (Figure 5B). On the contrary, both the basal and TGF-β1-induced α-SMA, COL1A1 as well as p-JNK and p-c-Jun expression were increased by in the PDCD4-knockdown LX-2 cells as compared to negative control group (Figure 5C and D), further supporting that PDCD4 is a potential inhibitor of HSC activation by regulating JNK signaling pathway.

## Amygdalin Upregulates PDCD4 by Regulating mTOR-S6K1 Signaling Pathway

To investigate the mechanism underlying the regulation of PDCD4 expression by amygdalin to inhibit HSC activation, we examined whether amygdalin transcriptionally regulated PDCD4 gene expression by RT-qPCR assay. Unexpectedly, neither amygdalin nor TGF-β1 altered the PDCD4 mRNA expression in the LX-2 cells (Figure 4A). It was previously reported that PDCD4 is degraded by proteasome via E3 ubiquitin ligase β-TrCP.<sup>43</sup> Therefore, LX-2 cells were treated with TGF-β1 and/or MG132 to determine whether the regulation of PDCD4 by TGF-β1 was proteasomal degradation-dependent. The downregulation of PDCD4 by TGF-β1 was restored by treatment with the proteasome inhibitor MG132

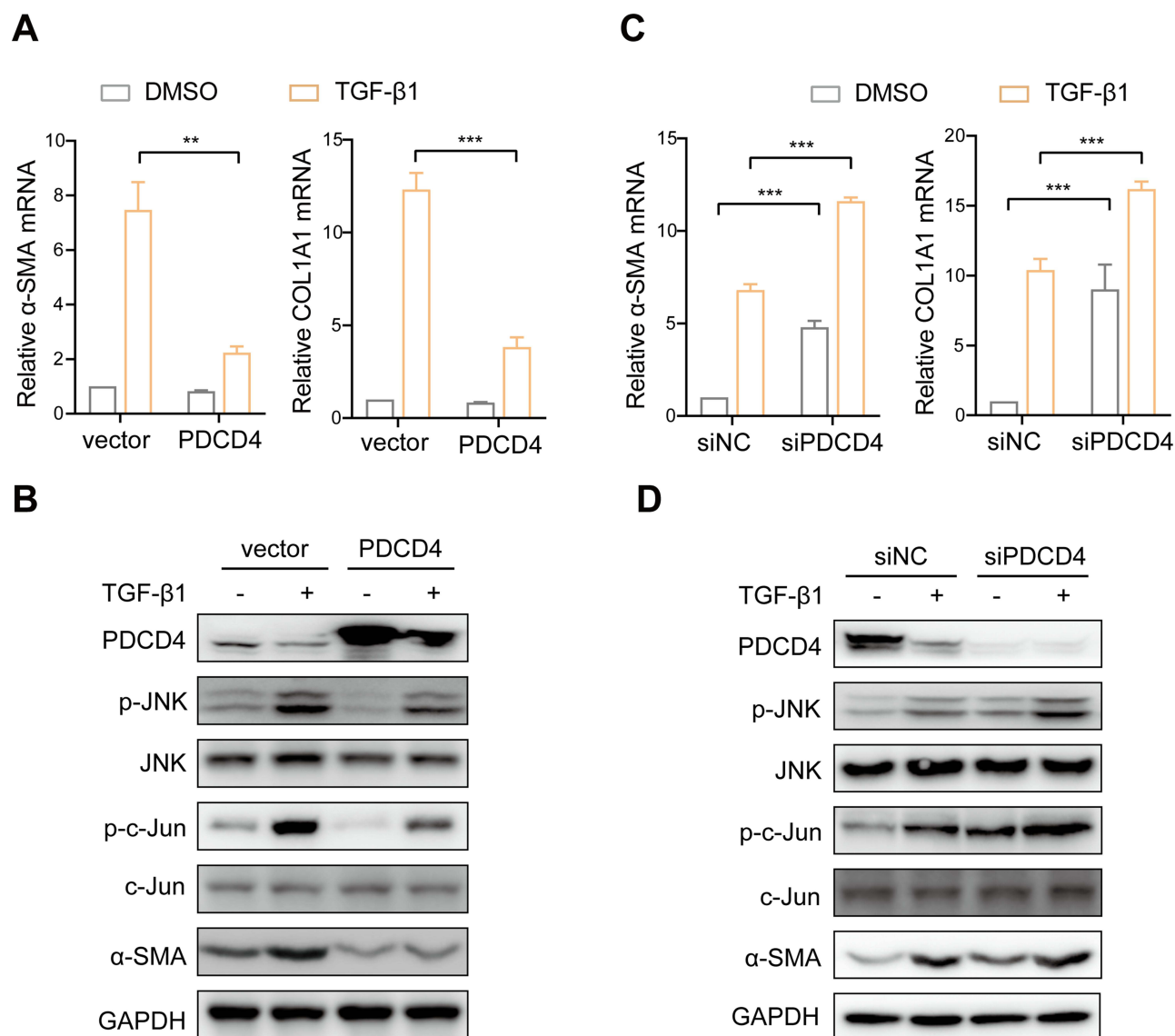


**Figure 5** Effects of PDCD4 on HSC activation and JNK/c-Jun signaling pathway activity. LX-2 cells were transfected with empty vector or PDCD4 plasmid or transfected with siNC or siPDCD4 for 48 h and stimulated with TGF- $\beta$ 1 for another 24 h. **(A and C)** Relative mRNA expression was measured by rt-qPCR for  $\alpha$ -SMA and COL1A1.  $n = 5$ , \*\* $P < 0.01$ , \*\*\* $P < 0.001$ . **(B and D)** The protein levels of total or phosphorylated JNK, c-jun,  $\alpha$ -SMA and COL1A1 were analyzed by Western blotting.

(Figure 6A). It has been reported that activation of the mTOR/S6K1 pathway was responsible for the phosphorylation and subsequent degradation of PDCD4.<sup>43,44</sup> Consistently, stimulation of LX-2 cells with TGF- $\beta$ 1 increased the phosphorylation of mTOR, S6K1 and PDCD4 but downregulated total PDCD4 expression in a time-dependent manner (Figure 6B), suggesting that TGF- $\beta$ 1 induce the degradation of PDCD4 by activation of mTOR-S6K1 pathways to phosphorylates PDCD4. We then examined the effect of amygdalin on the phosphorylation of PDCD4. As shown in Figure 6C, treatment of LX-2 with the amygdalin also prevented TGF- $\beta$ 1-induced downregulation of PDCD4 and upregulation of p-JNK and p-c-Jun as well as  $\alpha$ -SMA expression. Consistently, these changes were also observed in cells treated with selective mTOR inhibitor rapamycin. These results suggest that amygdalin prevents TGF- $\beta$ 1-induced PDCD4 downregulation by inhibiting the activation of mTOR/S6K1 pathways.

## Discussion

This study elucidates a mechanism by which amygdalin exerts anti-fibrosis effect, which helps to provide new targets for the treatment of liver fibrosis. Administration of amygdalin stabilizes the protein levels of the PDCD4 that was decreased

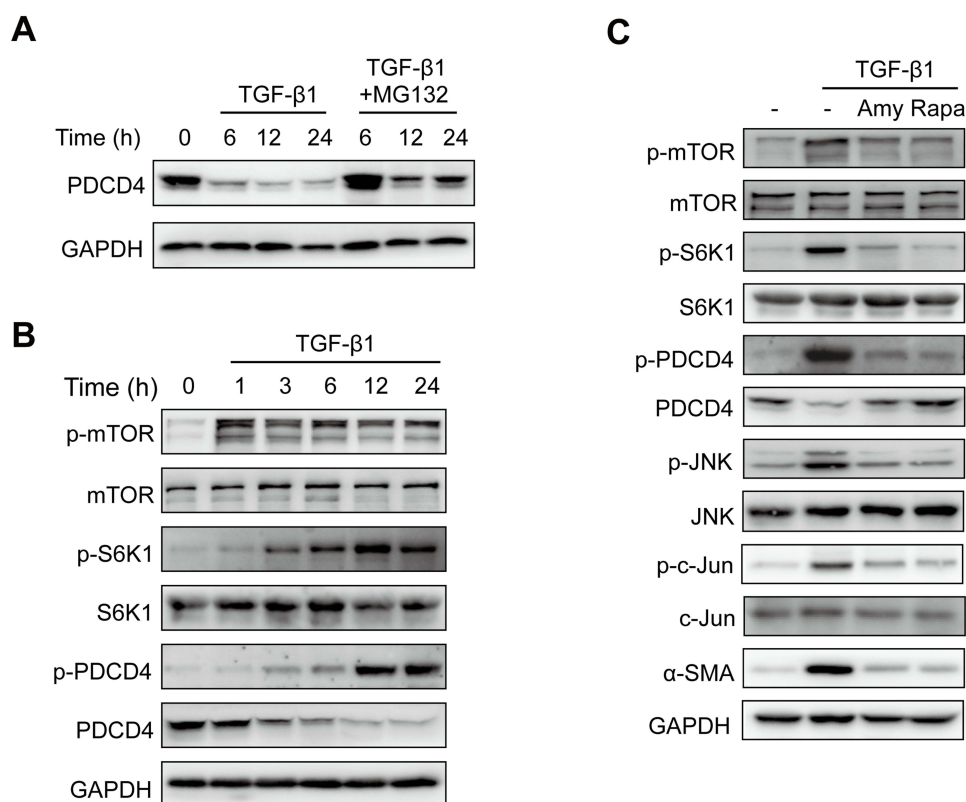


**Figure 6** Amygdalin upregulates PDCD4 via inhibiting activation mTOR/S6K1 signaling pathway. **(A)** LX-2 cells were stimulated with TGF-β1 for different time and MG132 for another 4 h. The protein level of PDCD4 was analyzed by Western blotting. **(B)** LX-2 cells were stimulated with TGF-β1 and the protein levels of total and phosphorylation levels of mTOR, S6K1 and PDCD4 were analyzed by Western blotting. **(C)** LX-2 cells were treated with amygdalin for 12 h or Rapamycin for 2 h and stimulated with TGF-β1 for another 24 h, and the protein levels of total and phosphorylated mTOR, S6K1, JNK, c-Jun were analyzed by Western blotting.

by fibrogenic factor TGF-β1. This effect is mediated by the negative regulation of mTOR/S6K1 signaling and downstream event of PDCD4 phosphorylation, thereby inhibiting PDCD4 proteasomal degradation.

PDCD4 is a tumor suppressor and has been found to lose expression in several cancers, including liver cancer. Overexpression of PDCD4 was shown to enhance sensitivity of cisplatin, paclitaxel, and carboplatin.<sup>45–47</sup> PDCD4 has also been reported to be inhibited by miRNA-21 in hepatocellular carcinoma.<sup>48</sup> In this study, we found that PDCD4 expression was repressed in TGF-β1-induced HSC cells and CCl<sub>4</sub>-fibrosis liver tissue. Low levels of PDCD4 significantly promoted α-SMA expression, while elevated levels of PDCD4 inhibited α-SMA and HSC activation, further confirming the important role of PDCD4 in the antifibrotic process.

Our proteomic and bioinformatic study indicated that amygdalin modulated the JNK cascade pathway, and subsequent functional experiment further showed that PDCD4 can suppress basal and TGF-β1-induced phosphorylation of JNK and c-Jun (Figure 5). The c-Jun N-terminal kinases (JNKs), as members of the MAPK family, mediate eukaryotic cell responses to a wide range of stimuli, such as oxidative stress, infection, inflammation and DNA damage.<sup>49</sup> Studies have indicated that PDCD4 can inhibit AP-1-dependent transcription through inhibition of the transactivation c-Jun and or interfering with its phosphorylation.<sup>40,42</sup> Additionally, PDCD4 can regulate the expression of upstream kinases of JNK (such as MAP4K1) or influence the expression of miRNA-21, thereby affecting the activation of JNK/c-Jun signaling.<sup>30,50,51</sup> And JNK inhibitors prevented TGF-β1-induced murine HSC activation and reduced fibrosis after being injected with BDL or CCl<sub>4</sub> by decreasing PDGF and TGFβ signaling.<sup>52</sup> Zhang et al also suggested that amygdalin protects against acetaminophen-induced acute liver failure by regulating JNK downstream signaling, thereby reducing inflammatory response and inhibiting hepatocyte death.<sup>53</sup> Therefore, our study suggest that PDCD4 may exert its anti-HSC activation effect by regulating the JNK signaling pathway.

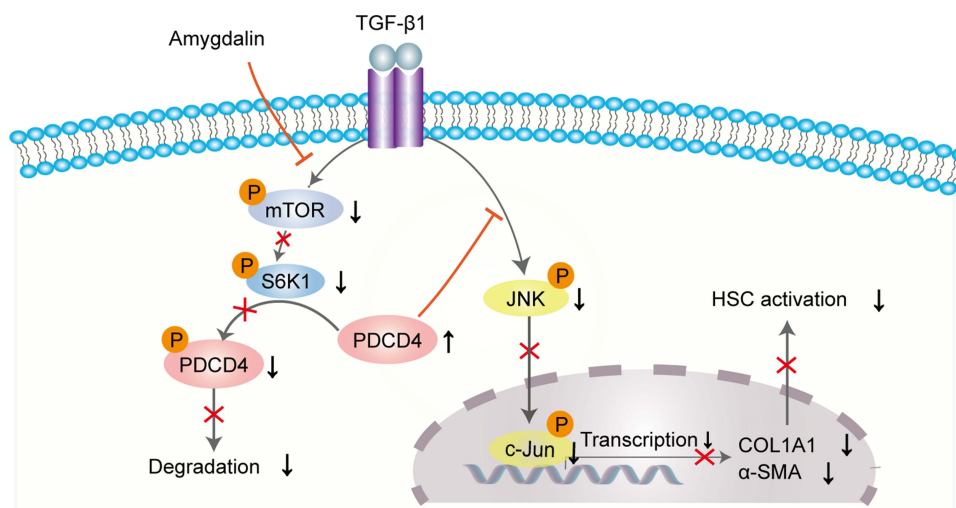


**Figure 7** Schematic revealing the mechanism underlying the protective effect of amygdalin against liver fibrosis.

PDCD4 expression can be regulated at transcription, translation and protein degradation levels.<sup>54</sup> Activation of S6K1 by mTOR signaling pathway leads to the phosphorylation of PDCD4 at Ser 67 and is subsequently degraded by the ubiquitin ligase  $\beta$ -TRCP.<sup>43</sup> Using computational modelling and simulation techniques, Ayaz et al reported that amygdalin had direct contribution to regulate PI3K-mTOR activities on various types of cancer.<sup>55</sup> In addition, mTOR/S6K1 activation was involved in collagen and fibronectin gene expression in human HSC, rapamycin treatment reduces experimental fibrogenesis.<sup>56,57</sup> Its inhibition has shown promise in reducing fibrogenesis, making it a potential therapeutic target.<sup>58,59</sup> Thus, it was reasonable to speculate that amygdalin may promote expression of PDCD4 and suppress HSCs activation by regulating mTOR-S6K1 axis. Indeed, our results indicated that mTOR/S6K1 activation was inhibited by amygdalin, which was accompanied by a decrease in PDCD4 phosphorylation at serine 67 and upregulation of PDCD4 expression (Figure 6C). Thus, our study provides another molecular mechanism that allows mTOR mediated-HSC activation.

Although our study demonstrates that amygdalin can significantly alleviate  $\text{CCl}_4$ -induced liver fibrosis, as evidenced by liver tissue staining (H&E, Masson, and  $\alpha$ -SMA), blood biochemical markers (AST and ALT), and the expression of fibrosis markers ( $\alpha$ -SMA and COL1A1), the relatively small sample size in the animal experiments may affect the robustness of the findings and the generalizability of the observed effects. In addition, this study did not explore the effects of amygdalin on TGF- $\beta$ /Smad signaling but focused on understanding the pleiotropic effects of TGF- $\beta$  and its downstream PDCD4-mediated regulatory mechanisms, which will contribute to design better TGF- $\beta$ -based therapeutics. Furthermore, this study has not yet clarified the direct and indirect roles of amygdalin in regulating PDCD4 expression and HSC activation, in order to better understand its protective effects in liver fibrosis. Future studies are needed to validate and expand our findings under different experimental conditions.

## Conclusion

In summary, our study showed that PDCD4 reduced HSC activation by regulating JNK/c-Jun signaling. Amygdalin, a cyanogenic glucoside derived from persicae semen, promotes the expression of PDCD4 by suppressing the phosphorylation of both the mTOR/S6K1 pathway and PDCD4, thereby inhibiting activation of HSCs (Figure 7). These results suggest that PDCD4 may be a promising therapeutic target for treating liver fibrosis and preliminarily elucidate the key molecular mechanisms underlying the pharmacological effects of Amygdalin.

## Abbreviations

ALT, Alanine Transaminase; AST, Aminotransferase;  $\text{CCl}_4$ , Carbon tetrachloride; ECM, Extracellular matrix; FASP, Filter-assisted sample preparation; FFPE, Formalin-fixed paraffin-embedded; GSEA, Gene Set Enrichment Analysis; GOBP, Gene Ontology Biological Process; HSCs, Hepatic stellate cells; IGF, Insulin-like growth factor; MMP-9, Matrix

Metalloproteinases-9; mTOR, Mechanistic target of rapamycin; JNK, N-terminal kinase; PDCD4, Programmed cell death protein 4; PDGF, Platelet-derived growth factor; S6K1, Ribosomal protein S6 kinase beta-1; TIMP-1, Tissue Inhibitor of Metalloproteinases 1; TGF- $\beta$ 1, Transforming growth factor-beta1.

## Data Sharing Statement

All results generated in the present study are included in this published article and [supplementary files](#). Other supporting datasets and processed data generated are available from the corresponding author on reasonable request. The Supporting Information for raw file of LC-MS/MS is available free of charge on the ProteomeXchange Consortium via the PRIDE partner repository with the data set identifier PXD050229.

## Acknowledgments

We thank the Institute of Liver Diseases, Shuguang Hospital affiliated to Shanghai University of Traditional Chinese Medicine for providing the practical help. We also thank the Institutional Technology Service Center of Shanghai Institute of Materia Medica for all the technical support. In addition, we thank Dr Alexey Kononikhin from the Skolkovo Institute of Science and Technology, Moscow, Russia, for his valuable suggestions and contributions to this study.

## Author Contributions

All authors made a significant contribution to the work reported, whether that is in the conception, study design, execution, acquisition of data, analysis, and interpretation, or in all these areas; took part in drafting, revising or critically reviewing the article; gave final approval of the version to be published; have agreed on the journal to which the article has been submitted; and agree to be accountable for all aspects of the work.

## Funding

This research was supported by the National Key Research and Development Program (Grant No. 2020YFA0509000), capital appropriations from the National Treasury (Grant No. E2G804H), and Shanghai Leading Talent Program of Eastern Talent Plan (Grant No. LJ2023123).

## Disclosure

The authors report no conflicts of interest in this work.

## References

- Asrani SK, Devarbhavi H, Eaton J, Kamath PS. Burden of liver diseases in the world. *J Hepatol*. 2019;70(1):151–171. doi:10.1016/j.jhep.2018.09.014
- Hams E, AvIELLO G, Fallon PG. The schistosoma granuloma: friend or foe? *Front Immunol*. 2013;4:89. doi:10.3389/fimmu.2013.00089
- Seki E, Schwabe RF. Hepatic inflammation and fibrosis: functional links and key pathways. *Hepatology*. 2015;61(3):1066–1079. doi:10.1002/hep.27332
- Parola M, Pinzani M. Liver fibrosis: pathophysiology, pathogenetic targets and clinical issues. *mol Aspects Med*. 2019;65:37–55. doi:10.1016/j.mam.2018.09.002
- Panda PK, Naik PP, Meher BR, et al. Corrigendum to “PUMA dependent mitophagy by abrus agglutinin contributes to apoptosis through ceramide generation” [Biochim. Biophys. Acta Mol. Cell Res. 1865 (2018) 480–495]. *Biochim Biophys Acta mol Cell Res*. 2019;1866(10):1689.
- Dooley S, Ten DP. TGF-beta in progression of liver disease. *Cell Tissue Res*. 2012;347(1):245–256.
- Moustakas A, Heldin CH. Non-Smad TGF-beta signals. *J Cell Sci*. 2005;118(Pt 16):3573–3584.
- Zhang YE. Non-smad pathways in TGF-beta signaling. *Cell Res*. 2009;19(1):128–139. doi:10.1038/cr.2008.328
- Zhang YE. Non-smad signaling pathways of the TGF-beta family. *Cold Spring Harb Perspect Biol*. 2017;9(2):a022129. doi:10.1101/cshperspect.a022129
- Dewidar B, Meyer C, Dooley S, Meindl-Beinker AN. TGF-beta in hepatic stellate cell activation and liver fibrogenesis-updated 2019. *Cells*. 2019;8(11). doi:10.3390/cells8111419
- He XY, Wu LJ, Wang WX, Xie PJ, Chen YH, Wang F. Amygdalin - a pharmacological and toxicological review. *J Ethnopharmacol*. 2020;254:112717. doi:10.1016/j.jep.2020.112717
- Blaheta RA, Nelson K, Haferkamp A, Juengel E. Amygdalin, quackery or cure? *Phytomedicine*. 2016;23(4):367–376. doi:10.1016/j.phymed.2016.02.004
- Albogami S, Hassan A, Ahmed N, et al. Evaluation of the effective dose of amygdalin for the improvement of antioxidant gene expression and suppression of oxidative damage in mice. *PeerJ*. 2020;8:e9232. doi:10.7717/peerj.9232

14. Porras M, Gomez LA, Perez JJ. Anti-inflammatory effect of amygdalin analogs following topical administration on the TPA-induced irritant contact dermatitis model in mice. *Exp Dermatol*. 2021;30(6):874–876. doi:10.1111/exd.14284
15. Shi H, Zheng G, Chen N. Amygdalin improves the renal function via anti-oxidation and anti-fibrosis in rats with chronic renal failure. *Panminerva Med*. 2020. doi:10.23736/S0031-0808.20.03977-4
16. Xiao Z, Ji Q, Fu YD, et al. Amygdalin ameliorates liver fibrosis through inhibiting activation of TGF-beta/Smad signaling. *Chin J Integr Med*. 2023;29(4):316–324. doi:10.1007/s11655-021-3304-y
17. Chen J, Hu Y, Mou X, Wang H, Xie Z. Amygdalin alleviates renal injury by suppressing inflammation, oxidative stress and fibrosis in streptozotocin-induced diabetic rats. *Life Sci*. 2021;265:118835. doi:10.1016/j.lfs.2020.118835
18. Sun X, Tan Y, Lyu J, Liu HL, Zhao ZM, Liu CH. Active components formulation developed from Fuzheng Huayu recipe for anti-liver fibrosis. *Chin J Integr Med*. 2022;28(6):538–544. doi:10.1007/s11655-021-3293-x
19. Hu XQ, Song YN, Wu R, et al. Metabolic mechanisms of Fuzheng-Huayu formula against liver fibrosis in rats. *J Ethnopharmacol*. 2019;238:111888. doi:10.1016/j.jep.2019.111888
20. Xu LM, Liu C, Liu P. Effect of amygdalin on proliferation of rat hepatic fat-storing cells and collagen production in vitro. *World J Gastroenterol*. 1997;3(2):103. doi:10.3748/wjg.v3.i2.103
21. Zhang C, Zhang D, Wang Y, et al. Pharmacokinetics and anti-liver fibrosis characteristics of amygdalin: key role of the deglycosylated metabolite prunasin. *Phytomedicine*. 2022;99:154018. doi:10.1016/j.phymed.2022.154018
22. Fu Y, Xiao Z, Tian X, et al. The novel Chinese medicine JY5 formula alleviates hepatic fibrosis by inhibiting the notch signaling pathway. *Front Pharmacol*. 2021;12:671152. doi:10.3389/fphar.2021.671152
23. Zhang LJ, Sun MY, Ning BB, et al. Xiayuxue decoction attenuates hepatic stellate cell activation and sinusoidal endothelium defenestration in CCl<sub>4</sub>-induced fibrotic liver of mice. *Chin J Integr Med*. 2014;20(7):516–523. doi:10.1007/s11655-014-1862-y
24. Tian H, Liu L, Li Z, et al. Chinese medicine CGA formula ameliorates liver fibrosis induced by carbon tetrachloride involving inhibition of hepatic apoptosis in rats. *J Ethnopharmacol*. 2019;232:227–235. doi:10.1016/j.jep.2018.11.027
25. Chen DQ, Feng YL, Cao G, Zhao YY. Natural products as a source for antifibrosis therapy. *Trends Pharmacol Sci*. 2018;39(11):937–952. doi:10.1016/j.tips.2018.09.002
26. Wang Q, Yang HS. The role of Pdc4 in tumour suppression and protein translation. *Biol Cell*. 2018;110(8):169–177. doi:10.1111/boc.201800014
27. Desai KM, Kale AD, Angadi PV, Datar UV, Belaldavar C, Arany PR. Role of programmed cell death 4 in myofibroblast differentiation in oral submucous fibrosis. *J Oral Maxillofac Pathol*. 2021;25(3):430–436. doi:10.4103/jomfp.jomfp\_86\_21
28. Yu L, Yang Y, Wang J, et al. PDCD4 promotes inflammation/fibrosis by activating the PPAR-gamma/NF-kappaB pathway in mouse atrial myocytes. *Mol Med Rep*. 2024;30(5). doi:10.3892/mmr.2024.13333
29. Perveen R, Ozaki I, Manirujjaman M, et al. Induction of premature senescence and a less-fibrogenic phenotype by programmed cell death 4 knockdown in the human hepatic stellate cell line Lieming Xu-2. *Hum Cell*. 2023;36(2):583–601. doi:10.1007/s13577-022-00844-9
30. Zhang Z, Zha Y, Hu W, et al. The autoregulatory feedback loop of microRNA-21/programmed cell death protein 4/activation protein-1 (MiR-21/PDCD4/AP-1) as a driving force for hepatic fibrosis development. *J Biol Chem*. 2013;288(52):37082–37093. doi:10.1074/jbc.M113.517953
31. Sun Q, Miao J, Luo J, et al. The feedback loop between miR-21, PDCD4 and AP-1 functions as a driving force for renal fibrogenesis. *J Cell Sci*. 2018;131(6). doi:10.1242/jcs.202317
32. Li Y, Pang J, Wang J, et al. Knockdown of PDCD4 ameliorates neural cell apoptosis and mitochondrial injury through activating the PI3K/AKT/mTOR signal in Parkinson's disease. *J Chem Neuroanat*. 2023;129:102239. doi:10.1016/j.jchemneu.2023.102239
33. Hao XJ, Xu CZ, Wang JT, et al. miR-21 promotes proliferation and inhibits apoptosis of hepatic stellate cells through targeting PTEN/PI3K/AKT pathway. *J Recept Signal Transduction Res*. 2018;38(5–6):455–461. doi:10.1080/10799893.2019.1585452
34. Fan Q, Lu Q, Wang G, et al. Optimizing component formula suppresses lung cancer by blocking DTL-mediated PDCD4 ubiquitination to regulate the MAPK/JNK pathway. *J Ethnopharmacol*. 2022;299:115546. doi:10.1016/j.jep.2022.115546
35. Thakur SS, Geiger T, Chatterjee B, et al. Deep and highly sensitive proteome coverage by LC-MS/MS without prefractionation. *mol Cell Proteomics*. 2011;10(8):M110–M3699. doi:10.1074/mcp.M110.003699
36. Wisniewski JR, Nagaraj N, Zougman A, Gnäd F, Mann M. Brain phosphoproteome obtained by a FASP-based method reveals plasma membrane protein topology. *J Proteome Res*. 2010;9(6):3280–3289. doi:10.1021/pr1002214
37. Jombart T. adegenet: a R package for the multivariate analysis of genetic markers. *Bioinformatics*. 2008;24(11):1403–1405. doi:10.1093/bioinformatics/btn129
38. Subramanian A, Tamayo P, Mootha VK, et al. Gene set enrichment analysis: a knowledge-based approach for interpreting genome-wide expression profiles. *Proc Natl Acad Sci U S A*. 2005;102(43):15545–15550. doi:10.1073/pnas.0506580102
39. Mootha VK, Lindgren CM, Eriksson KF, et al. PGC-1alpha-responsive genes involved in oxidative phosphorylation are coordinately down-regulated in human diabetes. *Nat Genet*. 2003;34(3):267–273. doi:10.1038/ng1180
40. Yang HS, Knies JL, Stark C, Colburn NH. Pdc4 suppresses tumor phenotype in JB6 cells by inhibiting AP-1 transactivation. *Oncogene*. 2003;22(24):3712–3720. doi:10.1038/sj.onc.1206433
41. Liu J, Zhai R, Zhao J, et al. Programmed cell death 4 overexpression enhances sensitivity to cisplatin via the JNK/c-Jun signaling pathway in bladder cancer. *Int J Oncol*. 2018;52(5):1633–1642. doi:10.3892/ijo.2018.4303
42. Bitomsky N, Bohm M, Klempnauer KH. Transformation suppressor protein Pdc4 interferes with JNK-mediated phosphorylation of c-Jun and recruitment of the coactivator p300 by c-Jun. *Oncogene*. 2004;23(45):7484–7493. doi:10.1038/sj.onc.1208064
43. Dorrello NV, Peschiaroli A, Guardavaccaro D, Colburn NH, Sherman NE, Pagano M. S6K1- and betaTRCP-mediated degradation of PDCD4 promotes protein translation and cell growth. *Science*. 2006;314(5798):467–471. doi:10.1126/science.1130276
44. Dennis MD, Jefferson LS, Kimball SR. Role of p70S6K1-mediated phosphorylation of eIF4B and PDCD4 proteins in the regulation of protein synthesis. *J Biol Chem*. 2012;287(51):42890–42899. doi:10.1074/jbc.M112.404822
45. Zhang X, Wang X, Song X, et al. Programmed cell death 4 enhances chemosensitivity of ovarian cancer cells by activating death receptor pathway in vitro and in vivo. *Cancer Sci*. 2010;101(10):2163–2170. doi:10.1111/j.1349-7006.2010.01664.x
46. Shiota M, Izumi H, Tanimoto A, et al. Programmed cell death protein 4 down-regulates Y-box binding protein-1 expression via a direct interaction with Twist1 to suppress cancer cell growth. *Cancer Res*. 2009;69(7):3148–3156. doi:10.1158/0008-5472.CAN-08-2334

47. Jansen AP, Camalier CE, Stark C, Colburn NH. Characterization of programmed cell death 4 in multiple human cancers reveals a novel enhancer of drug sensitivity. *mol Cancer Ther.* 2004;3(2):103–110.
48. Tomimaru Y, Eguchi H, Nagano H, et al. MicroRNA-21 induces resistance to the anti-tumour effect of interferon-alpha/5-fluorouracil in hepatocellular carcinoma cells. *Br J Cancer.* 2010;103(10):1617–1626.
49. Zeke A, Misheva M, Remenyi A, Bogoyevitch MA. JNK signaling: regulation and functions based on complex protein-protein partnerships. *Microbiol Mol Biol Rev.* 2016;80(3):793–835. doi:10.1128/MMBR.00043-14
50. Yang HS, Matthews CP, Clair T, et al. Tumorigenesis suppressor Pdc4 down-regulates mitogen-activated protein kinase kinase kinase 1 expression to suppress colon carcinoma cell invasion. *mol Cell Biol.* 2006;26(4):1297–1306.
51. Wang Q, Zhang Y, Yang HS. Pdc4 knockdown up-regulates MAP4K1 expression and activation of AP-1 dependent transcription through c-Myc. *Biochim Biophys Acta.* 2012;1823(10):1807–1814. doi:10.1016/j.bbamcr.2012.07.004
52. Kluwe J, Pradere JP, Gwak GY, et al. Modulation of hepatic fibrosis by c-Jun-N-terminal kinase inhibition. *Gastroenterology.* 2010;138(1):347–359. doi:10.1053/j.gastro.2009.09.015
53. Zhang C, Lin J, Zhen C, et al. Amygdalin protects against Acetaminophen-induced acute liver failure by reducing inflammatory response and inhibiting hepatocyte death. *Biochem Biophys Res Commun.* 2022;602:105–112. doi:10.1016/j.bbrc.2022.03.011
54. Matsuhashi S, Manirujjaman M, Hamajima H, Ozaki I. Control mechanisms of the tumor suppressor PDCD4: expression and functions. *Int J mol Sci.* 2019;20(9):2304.
55. Ayaz Z, Zainab B, Khan S, et al. In silico authentication of amygdalin as a potent anticancer compound in the bitter kernels of family Rosaceae. *Saudi J Biol Sci.* 2020;27(9):2444–2451. doi:10.1016/j.sjbs.2020.06.041
56. Svegliati-Baroni G, Ridolfi F, Di Sario A, et al. Intracellular signaling pathways involved in acetaldehyde-induced collagen and fibronectin gene expression in human hepatic stellate cells. *Hepatology.* 2001;33(5):1130–1140. doi:10.1053/jhep.2001.23788
57. Lei J, Li Q, Xu H, et al. Anlotinib improves bile duct ligation-induced liver fibrosis in rats via antiangiogenesis regulated by VEGFR2/mTOR pathway. *Drug Dev Res.* 2023;84(2):143–155. doi:10.1002/ddr.22019
58. Walker NM, Belloli EA, Stuckey L, et al. Mechanistic Target of Rapamycin Complex 1 (mTORC1) and mTORC2 as key signaling intermediates in mesenchymal cell activation. *J Biol Chem.* 2016;291(12):6262–6271.
59. Madala SK, Sontake V, Edukulla R, Davidson CR, Schmidt S, WD H. Unique and redundant functions of p70 ribosomal S6 kinase isoforms regulate mesenchymal cell proliferation and migration in pulmonary fibrosis. *Am J Respir Cell mol Biol.* 2016;55(6):792–803. doi:10.1165/rmb.2016-0090OC

## Drug Design, Development and Therapy

### Publish your work in this journal

Drug Design, Development and Therapy is an international, peer-reviewed open-access journal that spans the spectrum of drug design and development through to clinical applications. Clinical outcomes, patient safety, and programs for the development and effective, safe, and sustained use of medicines are a feature of the journal, which has also been accepted for indexing on PubMed Central. The manuscript management system is completely online and includes a very quick and fair peer-review system, which is all easy to use. Visit <http://www.dovepress.com/testimonials.php> to read real quotes from published authors.

Submit your manuscript here: <https://www.dovepress.com/drug-design-development-and-therapy-journal>

**Dovepress**  
Taylor & Francis Group